AGU PUBLICATIONS

JGR

Journal of Geophysical Research: Solid Earth

RESEARCH ARTICLE

10.1002/2014JB011294

Key Points:
- Holocene-age Mw 7.6–8.4 earthquake(s) in intraplate India
- Rift reactivation and continent-scale drainage diversion by active thrusting
- High stress-drop faulting and earthquake hazard in a plate interior

Correspondence to:
A. Copley,
acc41@cam.ac.uk

Citation:
Copley, A., S. Mitra, R. Alastair Sloan, S. Gaonkar, and K. Reynolds (2014), Active faulting in apparently stable peninsular India: Rift inversion and a Holocene-age great earthquake on the Tapti Fault, *J. Geophys. Res. Solid Earth*, *119*, doi:10.1002/2014JB011294.

Received 16 MAY 2014
Accepted 15 JUL 2014
Accepted article online 23 JUL 2014

Active faulting in apparently stable peninsular India: Rift inversion and a Holocene-age great earthquake on the Tapti Fault

Alex Copley[1], Supriyo Mitra[2], R. Alastair Sloan[3], Sharad Gaonkar[4], and Kirsty Reynolds[1]

[1]COMET, Bullard Laboratories, Department of Earth Sciences, University of Cambridge, Cambridge, UK, [2]Seismological Observatory, Department of Earth Sciences, IISER Kolkata, Mohanpur, India, [3]COMET, Department of Earth Sciences, University of Oxford, Oxford, UK, [4]Geological Survey of India (retired), Mumbai, India

Abstract We present observations of active faulting within peninsular India, far from the surrounding plate boundaries. Offset alluvial fan surfaces indicate one or more magnitude 7.6–8.4 thrust-faulting earthquakes on the Tapti Fault (Maharashtra, western India) during the Holocene. The high ratio of fault displacement to length on the alluvial fan offsets implies high stress-drop faulting, as has been observed elsewhere in the peninsula. The along-strike extent of the fan offsets is similar to the thickness of the seismogenic layer, suggesting a roughly equidimensional fault rupture. The subsiding footwall of the fault is likely to have been responsible for altering the continental-scale drainage pattern in central India and creating the large west flowing catchment of the Tapti river. A preexisting sedimentary basin in the uplifting hanging wall implies that the Tapti Fault was active as a normal fault during the Mesozoic and has been reactivated as a thrust, highlighting the role of preexisting structures in determining the rheology and deformation of the lithosphere. The slip sense of faults and earthquakes in India suggests that deformation south of the Ganges foreland basin is driven by the compressive force transmitted between India and the Tibetan Plateau. The along-strike continuation of faulting to the east of the Holocene ruptures we have studied represents a significant seismic hazard in central India.

1. Introduction

Although most continental earthquakes occur in relatively rapidly deforming regions between tectonic plates, it is widely recognized that rarer events also occur within areas traditionally thought of as rigid plates or “stable continental regions” [e.g., *Sykes*, 1978; *Johnston*, 1996; *Schulte and Mooney*, 2005]. Specific examples include earthquakes at Tennant Creek (Australia, 1988) [e.g., *McCaffrey*, 1989], New Madrid (USA, 1811–1812) [e.g., *Johnston and Schweig*, 1996], the Rann of Kachchh and Assam (India, 1819 and 1897) [e.g., *Bilham*, 1999; *Bilham and England*, 2001], Ungava (Canada, 1989) [e.g., *Adams et al.*, 1991], Manaus (Brazil, 1963) [e.g., *Assumpcao and Suarez*, 1988], and the Straits of Dover (UK/France, 1580) [e.g., *Neilson et al.*, 1984]. While earthquakes in these apparently stable regions are rare, the seismic hazard resulting from the uncommon events that do occur is significant for two main reasons. First, the interiors of very slowly deforming continental plates are generally thought to be cool [e.g., *Jaupart and Mareschal*, 1999] and often anhydrous [e.g., *Jackson et al.*, 2008], so earthquakes can occur to larger depths in a thicker seismogenic layer than in hotter and more active regions (e.g., >40 km [*Sloan et al.*, 2011]). Earthquakes in stable continental regions can therefore have large magnitudes if they rupture most of the seismogenic layer (e.g., $M_w \geq 8$; *Bilham and England* [2001]). Second, the long repeat times for earthquakes in slowly deforming regions can potentially lead to local populations being relatively unprepared for these unexpected events. One example is the 2001 M_w7.6 Bhuj (Gujarat) earthquake in NW India, which resulted in over 20,000 deaths in a relatively sparsely populated area. It is therefore worthwhile to study earthquakes and active faults in these slowly deforming regions of the continents, in order to increase our knowledge of the rare events that have occurred in the past and to identify faults on which earthquakes may occur in the future.

A second reason for studying the active deformation of low strain rate regions of the continents lies in attempting to constrain the material properties of the continental lithosphere. A wealth of techniques have been used to estimate the material properties of the seismic and aseismic parts of the lithosphere, including earthquake source studies, observations and models of interseismic strain accumulation and postseismic relaxation, borehole observations, and dynamic models of large-scale continental deformation. Due to the spatial distribution of earthquakes and geodetically measurable deformation, such studies have been mainly concerned with rapidly deforming lithosphere. The low rates of strain, and the scarcity of earthquakes, mean that considerably less is known about the largely aseismic areas of the continents. Although the analysis of postglacial relaxation provides information on Earth structure in some plate interiors [e.g., *Kaufmann and Lambek*, 2002], the large lateral extents of the ice loads means that these studies are more sensitive to the sublithospheric mantle. Studies based on the analysis of gravity anomalies, and the depth distributions of earthquakes and seismic velocity contrasts, imply the existence of important lateral variations in continental rheology [e.g., *Maggi et al.*, 2000a; *Simons and van der Hilst*, 2002]. A second reason for studying the deformation of low strain rate regions of the continents therefore lies in attempting to provide a more complete picture of the lateral variations in continental rheology.

In order to address these questions, this paper examines a region of active faulting within the Indian peninsula, far from the surrounding plate boundaries and rapidly deforming mountain ranges. We first summarize what is known about the active deformation of the Indian subcontinent and then describe field and remote sensing observations of Holocene-age active faulting on the Tapti Fault in Maharashtra state in western India. The effects of this faulting on the geomorphological evolution of the region are summarized before we discuss the implications for the properties and behavior of the Indian lithosphere and the forces driving the deformation.

2. Active Deformation of the Indian Subcontinent

This section introduces what is currently known about the active deformation of the Indian subcontinent. The hypotheses regarding the forces driving the deformation will be discussed later, in light of the results presented in this paper.

One major source of information regarding the deformation of India is seismic observations of earthquakes that have occurred during the modern instrumental period. We focus on earthquakes occurring within the lithosphere of peninsular India and not events within the bounding mountain ranges, on their range fronts, or within Indian material that has underthrust those ranges. Focal mechanisms of earthquakes within the subcontinent are shown in Figure 1. Seismicity occurs throughout the thickness of the crust and potentially into the very uppermost mantle [e.g., *Mukherjee*, 1942; *Chen and Molnar*, 1990; *Chen and Kao*, 1996; *Mitra et al.*, 2005; *Craig et al.*, 2012]. Seismicity in the lower crust, at temperatures which are likely to be up to $\sim 600°$C, has been interpreted to mean the lower crust is likely to be strong and anhydrous; otherwise ductile deformation would be expected at those temperatures [e.g., *Mackwell et al.*, 1998; *Jackson et al.*, 2008]. Beneath the Ganges foreland basin, normal faulting at shallow depths ($\leq$20 km) is underlain by deeper thrust faulting, probably due to the bending of the Indian lithosphere as it underthrusts the Tibetan Plateau. In northeast India, thrust and strike-slip faulting occur near the Shillong Plateau and Indo-Burman Ranges (SP and IBR in Figure 1). Throughout the remainder of the subcontinent, the faulting is dominantly thrust faulting on planes striking within 45° of E-W, with the exception of two oblique strike-slip events at latitudes of 15–20° (Figure 1). The largest earthquake to strike the subcontinent in the modern instrumental period was the 2001 M_w7.6 Bhuj (Gujarat) thrust-faulting earthquake in northwest India (labeled in Figure 1) [e.g., *Wesnousky et al.*, 2001; *Antolik and Dreger*, 2003; *Chandrasekhar et al.*, 2004; *Schmidt and Burgmann*, 2006; *Copley et al.*, 2011].

Historical accounts, field observations, and the reanalysis of geodetic surveys from the nineteenth century have provided information about two large events marked by stars in Figure 1: the 1819 magnitude 7.7 Rann of Kachchh and 1897 magnitude 8.1 Assam (Shillong Plateau) earthquakes [*Bilham*, 1999; *Bilham and England*, 2001]. These events both occurred on roughly E-W striking thrust faults. The longer historical catalogue [e.g., *Rao and Rao*, 1984; *Szeliga et al.*, 2010] reveals earthquakes distributed throughout the peninsula, shown by grey circles in Figure 1 (which have magnitudes of 4–8 and are likely to have location uncertainties of $\geq$50 km; *Szeliga et al.* [2010]). A number of authors [e.g., *Rao*, 2000; *Rajendran*, 2000] have noted that many Indian earthquakes are associated with preexisting structural features, such as an abandoned rift in the case of the Bhuj and Rann of Kachchh events. However, events not clearly associated with known preexisting structures have also occurred, such as the 1993 Killari earthquake [*Seeber et al.*, 1996]. A number of recent earthquakes have occurred along the ENE-WSW trending Narmada-Son Lineament, a long-recognized Precambrian tectonic feature that has been reactivated multiple times [e.g., *West*, 1962;

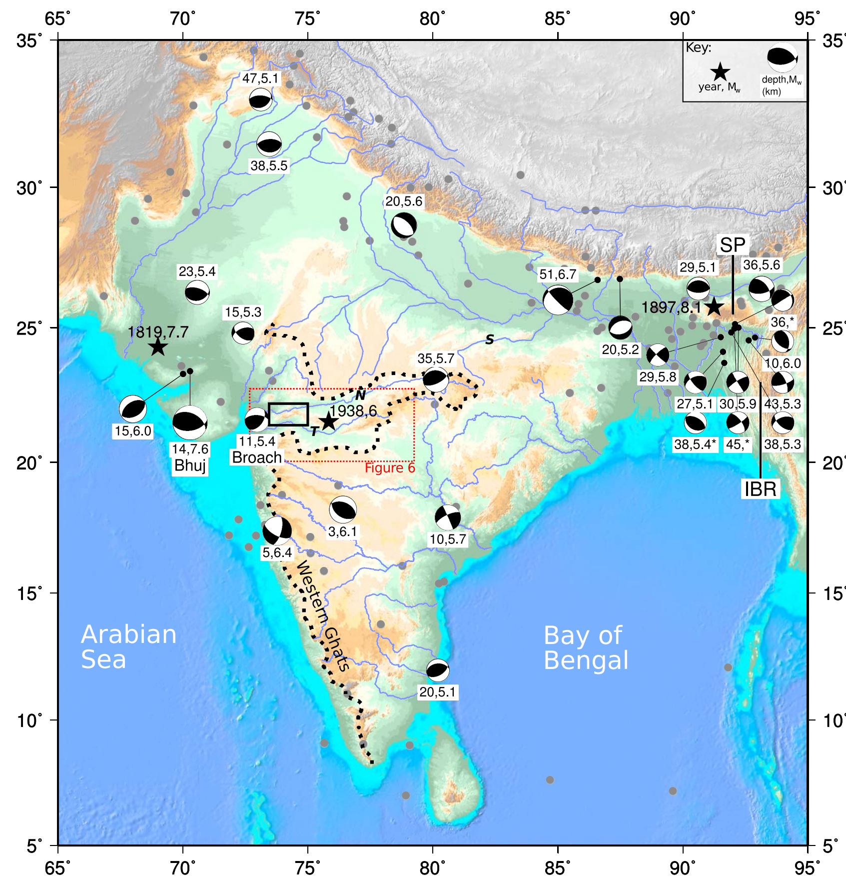

Figure 1. Topography and seismicity of the Indian subcontinent. Earthquake focal mechanisms are shown for events that occurred within Indian lithospheric material, and do not include those on the range fronts or within the bounding mountain ranges, or where Indian material underthrusts those ranges [*Langston*, 1976; *Chandra*, 1977; *Molnar et al.*, 1977; *Ni and Barazangi*, 1984; *Chen and Molnar*, 1990; *Chung*, 1993; *Chung and Gao*, 1995; *Seeber et al.*, 1996; *Chen and Kao*, 1996; *Maggi et al.*, 2000b; *Jackson*, 2002; *Mitra et al.*, 2005; *Priestley et al.*, 2008; *Copley et al.*, 2011]. Earthquakes are labeled with the centroid depth in kilometers and the moment magnitude. In NE India the magnitude marked with an asterisk is a body wave magnitude; the two with an asterisk but no magnitude date from the 1960s, and no magnitude was estimated by *Chen and Molnar* [1990]. Large black stars represent some significant earthquakes prior to the modern instrumental period, labeled with the date and magnitude and discussed in the text. Grey circles show earthquakes prior to 1970 in the catalogue of *Szeliga et al.* [2010], dating back to the mid-eighteenth century. The dotted black line shows the drainage divide in central and southern India between rivers flowing to the Arabian Sea and Bay of Bengal. *T*, *N*, and *S* mark the Tapti, Narmada, and Son rivers. The black box shows the location of Figure 2, and the red dotted box outlines the area of Figure 6.

Choubey, 1971; *Biswas*, 1982] and which roughly coincides with the courses of the Narmada and Son rivers (labeled N and S in Figure 1).

With the exception of the Shillong Plateau, modern geodetic techniques have been unable to identify the location and rate of strain accumulation on faults south of the Himalayas, due to the low rates of deformation. However, bounds have been placed on the possible rates of deformation across the entire subcontinent. *Bettinelli et al.* [2006] used GPS data to suggest that the internal compression of India was $\leq$2 mm/yr. *Banerjee et al.* [2008] used data from additional GPS sites and suggested a similar rate of 2 ± 1 mm/yr of north-south shortening. Their data are consistent with the shortening being concentrated in central India, in our region of focus in this paper, but did not allow the location of the strain to be robustly determined.

In order to provide further information about the active deformation of peninsular India, we have examined the tectonic geomorphology in part of central India. The signatures of past earthquakes preserved in the landscape can give insights into active faulting on timescales longer than the instrumental and historical records, which is particularly important in regions where the combination of low rates of deformation and large earthquakes means that repeat times are likely to be very long (e.g., upward of thousands of years). We focus on the Tapti Fault in western India (black box in Figure 1), where evidence of faulting is clearly visible in the geomorphology. Additionally, this region of India is where *Vredenburg* [1906] suggested the presence of Quaternary deformation based upon irregularities in the gradients of the rivers draining the area (as discussed below) and so warrants a detailed inspection.

3. Holocene Activity on the Tapti Fault

This section focuses on the Tapti Fault, in the area of western central India marked by the black box in Figure 1. We describe the geomorphological evidence for Holocene activity on the fault and estimate the likely magnitude of the earthquake(s) that produced the observed fault scarps.

The Tapti Fault cuts Deccan flood basalts and Cenozoic alluvium at the surface and strikes ENE-WSW. It is situated between the M_w5.4 1970 Broach earthquake that occurred ~100 km to the west [*Chung*, 1993] and the 1938 magnitude ~6 Satpura earthquake ~150 km to the east [*Mukherjee*, 1942] (both labeled in Figure 1). Teleseismic depth phases from the Satpura event, arriving 11 s after the first *P* arrival [*Mukherjee*, 1942], suggest that the source depth was 30–40 km, providing a minimum estimate for thickness for the seismogenic layer in this location which is consistent with earthquakes throughout the subcontinent [e.g., *Chen and Molnar*, 1990; *Chen and Kao*, 1996; *Mitra et al.*, 2005; *Craig et al.*, 2012]. The Tapti Fault is near the western end of the Narmada-Son Lineament and has been previously identified [e.g., *Jain et al.*, 1995; *Geological Survey of India*, 2000], although its recent activity has not been examined in detail. In this section we present new field observations of the Holocene activity of the Tapti Fault, located along the range front at the northern edge of the Tapti river valley.

3.1. The Central Section of the Fault

The topography in the region of the Tapti Fault is shown in Figure 2. A mountain range (the western section of the Satpura range) with peaks up to ~1300 m high lies immediately north of the fault and a low-lying (100–200 m) alluvial plain to the south. The topography of the mountains is asymmetric, with a steep southern slope and a gentle northern side, where the topography dies out over a distance of ~50 km. This distance is similar to the thickness of the seismogenic layer, as has been discussed for dip-slip faulting elsewhere [e.g., *Jackson and White*, 1989; *Scholz and Contreras*, 1998].

We examined in the field a number of locations on the southern range front of the mountains. Figure 3 shows the topography and an optical satellite image of an area near the village of Bandhare, labeled B in Figure 2. A river exiting the mountains has deposited an alluvial fan across the fault. We observed a vertical offset in the fan surface along a linear step that lies along strike from the range front to either side of the valley (Figure 3). We surveyed a topographic profile across this step, using GPS to estimate the horizontal locations of measurement points and the atmospheric pressure to estimate the elevation. This method is not sensitive to the absolute elevation, as the atmospheric pressure can be affected by meteorological conditions in addition to elevation, but when profiles are taken over a short time period the relative elevations are well constrained. We repeated profiles in uphill and downhill directions and on 2 days (once in the morning and once in the late afternoon). We found that the repeatability of elevation changes along the entire length of the profile, as distinct from the poorly constrained absolute elevation, was 1–2 m. We confirmed the elevation differences between multiple points along the profiles by simultaneous angle measurements using an Abney level and found agreement to within 0.5° (close to the measurement accuracy of the instrument) with no consistent sense of overestimate or underestimate. We have set the absolute elevations of the upper ends of our elevation profiles to the values of the nearest SRTM (Shuttle Radar Topography Mission; *Farr and Kobrick* [2000]) data points. To test the accuracy of our measurements, we can then compare our elevation values elsewhere on the profiles with the sparser SRTM data points (which have a horizontal posting of 90 m). An example is shown in Figure 3c. The SRTM data from the locations nearest to our elevation profile are shown as green circles, and our measurements are shown in black. This comparison demonstrates that our methods are able to accurately measure the topographic variation within a region and provide more detailed information than the sparser SRTM data.

A topographic profile across the step in the fan surface at Bandhare is shown in Figure 3c, showing a clear ~15 m vertical offset. The land is now farmed, but the optical satellite image dating to December 2002 shown in Figure 3b demonstrates that the topographic step was present prior to the onset of farming. In

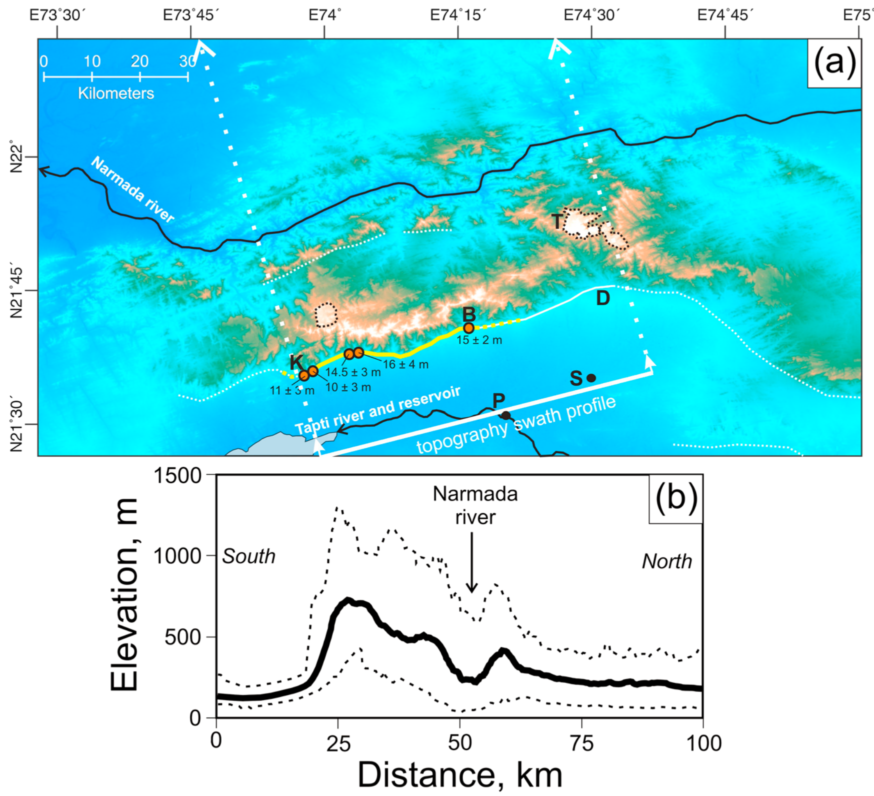

Figure 2. (a) Topography of the Tapti Fault. Orange circles show locations of fan offsets, with the vertical displacement indicated. The yellow line shows the inferred along-strike extent of the earthquake(s) that produced the fan displacements. The thin solid white line shows the part of the fault visited where no fan offsets were observed. Thin dotted white lines show faults inferred in the landscape based on remote sensing data but not visited during our fieldwork. T: Toranmal; D: Dhawadi; B: Bandhare; K: Kolavi; S: Shahada; P: Prakasha. (b) Topographic profile using data from within the thick white dotted lines on Figure 2a, stacked along strike. The dashed lines show the maximum and minimum topography, and the solid line the mean.

addition, the farming involves planting on the low-gradient fan surface, rather than the production of leveled fields, and there was no evidence in this location of topographic steps across field boundaries of more than a few centimeters in height (compared with the ~15 m step we are discussing). The major rivers running from the mountains into the valley incise along much of their lengths, as is seen throughout northern India (discussed below). However, there is a marked change in incision along the line of the fan offset, with minor streams incising steep-sided gullies into the higher part of the fan. We interpret the sharp topographic step to represent an offset due to faulting since the deposition of the fan surface, which is now vegetated and inactive. The appreciable gradient in the fan surface, which is the same above and below the topographic step, further implies that the scarp was produced by faulting, as a river terrace riser would be expected to be flanked by flat surfaces. Additionally, there is no nearby river with a course that would result in the construction of terraces with E-W striking risers.

A section through the fan created by excavations for a reservoir outflow in the location shown in Figure 3b allows the internal structure of the topographic step to be examined. On the north side of the step, Deccan basalts are overlain by a ~6 m thick sequence of bedded fan material above a subhorizontal erosional contact. The excavated outflow cuts through the fan material down to the basalt bedrock. The excavations coincide with the along-strike projection of the topographic step and include a zone of heavily altered basalts with plentiful white veining, dominantly striking subparallel to the fault. Much of the vein material is too weathered to reliably identify, but some crystals of quartz were found. The contact between the basalt and the fan material is displaced vertically by 10–20 m across this region of altered basalt. We interpret the altered and heavily veined basalt to mark the surface projection of the fault that produced the step in the fan surface and the equivalent offset in the basalt-fan contact. The lack of a single well-defined fault plane suggests that any surface ruptures during earthquakes on the Tapti Fault are likely to take the form of

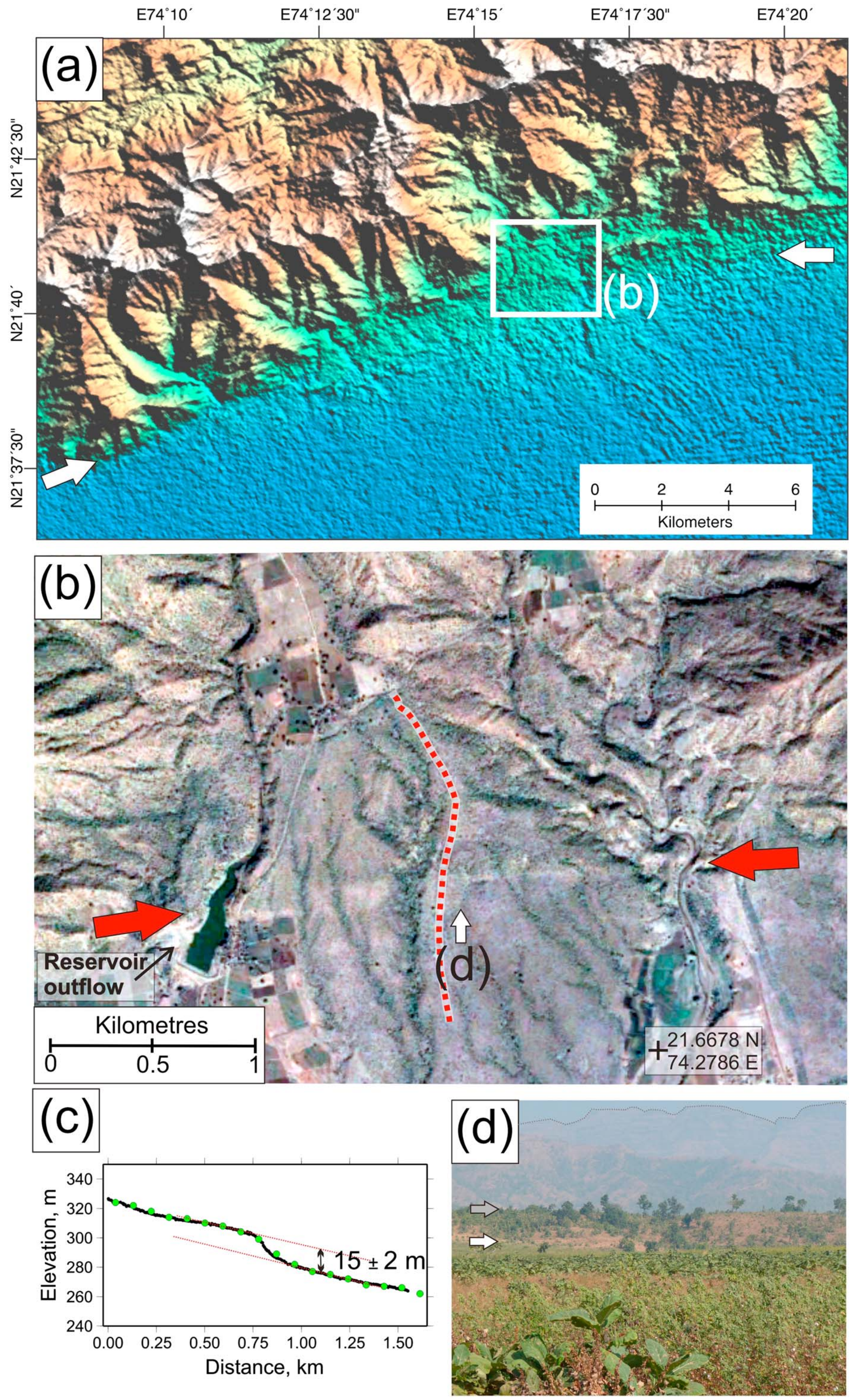

Figure 3. (a) Topography from the central section of the Tapti Fault, near Bandhare (labeled B in Figure 2). (b) Ikonos satellite image of the area shown by the white box in Figure 3a, acquired on 14 December 2002. Image copyright Google Earth and DigitalGlobe. The red arrows show the location of a topographic step crossing an alluvial fan. (c) The black points show the topographic profile along the red dotted line in Figure 3b, projected onto a north-south line. Green circles are SRTM data points. (d) Photograph of the step in the fan surface, from the location and direction marked in Figure 3b. The grey and white arrows mark the top and bottom of the scarp. The thin dotted black line marks the crest of the mountains to the north.

distributed deformation over a wide zone, as has been observed elsewhere (e.g., the 1980 El Asnam and 1988 Spitak earthquakes [*Yielding et al.*, 1981; *Philip et al.*, 1992]). Unfortunately, no distinctive features were visible in the basalt to allow the total offset across the altered and veined zone to be estimated. The presence of basalt on both sides of the fault, and the implications of this observation for the total displacement, is complicated by the presence of minor topography south of the fault, which may imply more than one strand in this location.

3.2. The Western Section of the Fault

We examined four locations to the west of Bandhare and measured topographic steps across alluvial fan surfaces (shown by orange circles in Figure 2). Incising rivers reveal geological structures similar to those described above. North of the topographic steps, 5–15 m sequences of bedded fan material overlie basalt, with subhorizontal erosional contacts between. In the region of the topographic steps, heavily altered and veined basalt was observed in the beds of incising rivers. No basalt was observed south of the fan offsets, with the altered basalt transitioning laterally into fan deposits, but the maximum depth of incision south of the fault was only ~10 m.

Figure 4 shows an example of a fan offset, from near the village of Kolavi (marked "K" in Figure 2). Uplift on a scarp across an alluvial fan surface, continuous with the range front to either side, has produced a similar topographic step to that described at Bandhare further east. An incising river (now dammed) allows the topographic step to be easily observed in profile (Figure 4c).

3.3. The Eastern Section of the Fault

We examined the range front to the east of the faulting described above, on the section of the fault shown by the solid white line in Figure 2. We did not observe topographic offsets in the alluvial fan surfaces, and none are visible in optical or topographic satellite data. Near the village of Dhawadi, marked D in Figure 2, a river with a large catchment in the mountains to the north has incised a 20–30 m deep gorge through the range front and into the plains to the south. North of the range front, basalt is overlain by 10–15 m of bedded fan material along a subhorizontal erosional contact, as was also observed along the sections of the fault examined further west. The excellent exposure allowed us to observe a ~200 m wide region along strike from the range front in which heavily altered and veined basalt is cut by multiple planes dipping north at 30–50°. These planes are formed of layers up to 5 cm thick containing clays, quartz, and clasts of basalt, and are likely to represent fault planes (although the weathered and homogeneous nature of the basalts means that no offset structures can be identified). Between the faults are extensive regions of basalt blocks wrapped by anastamosing clay-rich bands. To the south of this faulted basalt, the river section is composed entirely of bedded fan material with a thickness of 20–30 m. There is no disruption to the gentle dip of the upper surface of the fan on either side of the river gorge. This locality therefore represents the same geological situation as seen further west, with the altered and veined (and in this case visibly faulted) basalt at the range front representing the surface expression of the Tapti Fault. However, in this region, unlike further west, no fault motion appears to have occurred since the deposition of the most recent fan surface preserved to either side of the incising river gorge.

3.4. Sense of Motion on the Fault

In the regions where we observed topographic steps in the fan surfaces, the faulting in the underlying basalt does not take the form of a single, well-defined, fault plane. The motion at the surface appears to be accommodated in a broad zone of altered and veined basalt. It is therefore not possible to observe the dip direction of the fault and so establish the sense of the causative fault slip. However, information from along strike of the area of fan offsets allows us to infer the style of faulting. On the eastern section of the fault, near the village of Dhawadi (marked D in Figure 2), north dipping fault planes were observed in a river gorge at the range front. If the faulting on the central and western parts of the fault shares this dip, as seems likely, the fault motion that produced the fan offsets was thrust faulting. One hundred kilometers to the west of the Tapti Fault, the M_w5.4 Broach earthquake occurred in 1970 (marked in Figure 1). *Chung* [1993] analyzed the seismic waveforms of the event and obtained a thrust-faulting mechanism with a centroid depth of 11 km (i.e., in the top third of the seismogenic layer). This mechanism implies that the upper part of the crust in this region of India is under compression, in agreement with the thrusting sense of motion inferred based on the northward dip of the fault planes at the eastern end of the fault. We therefore suggest that the fan offsets were produced by thrust faulting.

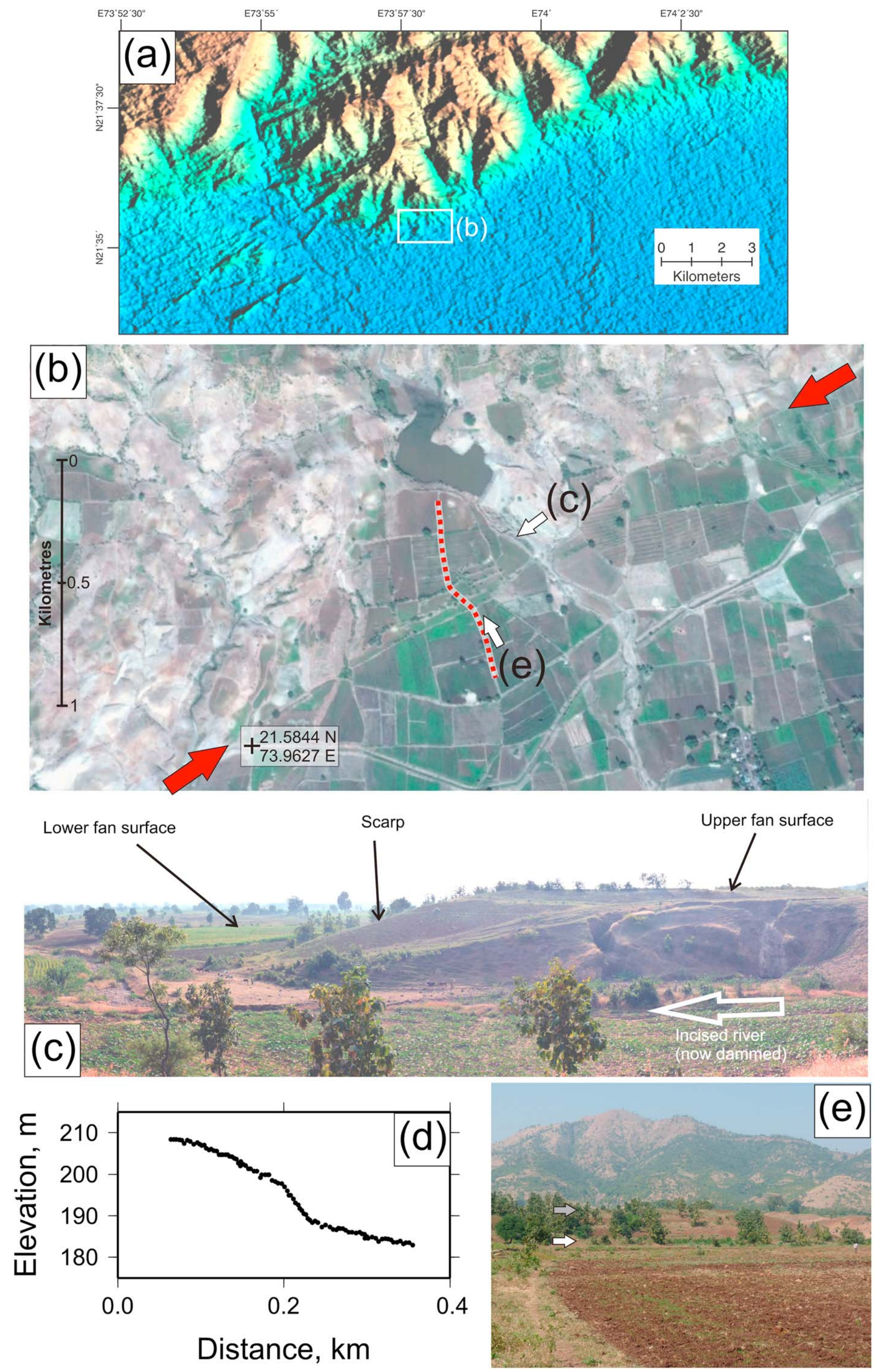

Figure 4. (a) Topography from the eastern section of the Tapti Fault, near Kolavi (marked K in Figure 2). (b) WorldView satellite image of the area inside the white box in Figure 4a. Image copyright Google Earth and DigitalGlobe. The range front is clearly visible and marked by red arrows. (c) Photograph of the profile of the fan offset, viewed across an incised river channel emerging from the mountains (now dammed), from the location and direction marked in Figure 4b. (d) Topographic profile along the red dotted line in Figure 4b, projected onto a line perpendicular to the range front. (e) Photograph of the front of the scarp, from the location and direction marked in Figure 4b. The grey and white arrows mark the top and bottom of the scarp.

3.5. Estimated Earthquake Magnitude

The ability to estimate a magnitude for the earthquake(s) that generated the fan offsets depends upon making assumptions about whether the motion occurred in one or multiple events. We have observed vertical offsets of 10–15 m along a 40–50 km section of fault. The 2001 M_w7.6 Bhuj thrust-faulting earthquake in the Indian lithosphere ∼450 km to the WNW had maximum slip of ∼14 m on a fault segment ∼35 km long [e.g., *Copley et al.*, 2011]. By analogy with that event, which had a similar amount of slip on a similar length rupture, the topographic steps we observe may have formed in a single event. In this case, and assuming the event ruptured to a depth of 20–40 km on a fault dipping at 30–60° (in keeping with modern Indian earthquakes), with slip required to produce a 15 m vertical offset on a fault 40–50 km long, the corresponding seismic moment would be 6.4×10^{20} to 4.8×10^{21} Nm (if the shear modulus is 4×10^{10}Pa). These values are equivalent to moment magnitudes of 7.8–8.4, in a similar range to the 7.6 Bhuj, 7.7 Rann of Kachchh, and 8.1 Assam events [*Bilham*, 1999; *Bilham and England*, 2001; *Copley et al.*, 2011]. If the topographic steps we have observed formed in more than one event (either separated along strike, or multiple events rupturing the same section of fault), the magnitudes would be correspondingly lower, for example, two events of M_W7.6–8.2. However, because we only observed a single scarp in the fans, and by analogy with the Bhuj event, we think the offsets were probably produced by a single earthquake. No events of such large magnitudes are known from historical or instrumental records in this location [e.g., *Rao and Rao*, 1984; *Martin and Szeliga*, 2010], suggesting that the fault slip which caused the fan offsets happened prior to the period for which historical records have been analyzed in detail (<1000 years).

In the above analysis we have neglected the possible role of postseismic afterslip and interseismic creep in generating the observed offsets. In general, the moment release in afterslip is a small proportion of the coseismic moment, with the 2004 Parkfield earthquake being a notable exception in which there was as much afterslip as coseismic motion [e.g., *Bruhat et al.*, 2011]. The uncertainty in our estimated moments resulting from the possible presence of afterslip is therefore less than that arising from the unknown number of earthquakes that produced the fan offsets and the range of possible values for the fault dip and depth extent of slip. It is unlikely that the fan offsets were produced entirely by interseismic creep, as in that case the production of offsets with a displacement-length ratio similar to nearby earthquakes would be highly coincidental.

3.6. Age of the Fan Offsets

We attempted to find material to date the deposition of the alluvial fan surfaces we studied. Unfortunately, the location of the fault in the Deccan basalts means that there is insufficient quartz or potassium feldspar in the sediments to attempt optically stimulated luminescence dating. The heavily vegetated surface means that changing levels of cosmogenic ray exposure through time, and the disruption of the shallow sediment by biological reworking, would result in ambiguous results from exposure dating. We only found two samples of organic material within the fan sediments, a testament to the rates of decay of organic material in the hot, monsoonal climate. These samples were burnt plant material, which we interpreted to be roots because they wrapped around clasts in the fan material. Carbon-14 dating showed them to be modern, suggesting that root material in this location can burn to a depth of >4 m below the ground surface.

Dating results from more amenable fan material in the surrounding areas of lowland India, beyond the extent of the Deccan basalts, allow us to infer the age of the offset fan surfaces at the Tapti Fault. A similar pattern of river incision and alluvial fan abandonment is seen throughout large parts of peninsular India. Dating of the abandoned and incised fan surfaces reveals a roughly synchronous date of fan abandonment and the onset of incision at ∼10–15 ka [e.g., *Srivastava et al.*, 2001; *Jain and Tandon*, 2003; *Gibling et al.*, 2005; *Williams et al.*, 2006]. This transition is interpreted to mark the change to a warmer and wetter climate and the strengthening of the summer monsoon. Such a change in climate will have led to increased river discharge, a resulting increase in erosional power, and therefore the incision of rivers and a shift of deposition to further downstream. Based on the regional agreement in the age of this fluvial transition, we infer an age of 10–15 ka for the abandonment of the alluvial fans we have studied. The fault offset we have observed is therefore likely to have occurred since this date. Additionally, it is likely that there has been no significant fault movement on the eastern part of the fault, in the area of uninterrupted fan surfaces, since ∼10–15 ka.

Figure 5. Panoramic photograph of the northwestern margin of the low-relief landscape at Toranmal (T in Figure 2), split onto two panels for clarity. On the left of the image is a low-relief landscape with low-gradient meandering rivers (not visible). On the right, the dramatic cliffs and deeply incised valleys on the margins of the gentle landscape are visible.

4. Regional Geomorphology and the Total Offset on the Tapti Fault

4.1. Post-Deccan Fault Offset

The lack of distinctive offset layers in the Deccan volcanics prevents the total fault offset since the emplacement of these rocks from being directly measured. However, in two locations, low-relief landscapes can be seen near the crest of the mountains north of the fault, shown by black dotted outlines in Figure 2. At Toranmal on the eastern of these landscapes (labeled T in Figure 2) we observed a low-relief landscape with meandering drainage at an elevation of ∼1000 m, surrounded by steep slopes and incising river valleys as deep as ∼400 m (Figure 5). These low-relief regions are likely to represent fragments of the prefaulting landscape that have been uplifted by fault motion and are being actively eroded along their edges, much like those seen in other tectonically active regions [e.g., Mongolia; *Jolivet et al.*, 2007]. The lack of marine sediments on the uplifted landscapes and the presence of basalt in river beds at Prakasha and Shahada (Marked P and S in Figure 2) suggest a total vertical offset on the fault of 500–1500 m since the emplacement of the Deccan volcanics. This estimate assumes that there was negligible prefaulting topography, in keeping with the remainder of the central Indian plateau. The wide range of suggested offsets partly arises from uncertainties in projecting to the fault the elevations of the low-relief landscape in the hanging wall and the basalt bedrock in the footwall. Our estimated offset is consistent with the 2–3° dip of back-tilted layers in the Deccan succession in the Tapti Fault hanging wall, if these were emplaced horizontally. We note that this estimate corresponds to the fault offset since the emplacement of the Deccan volcanics, and the fault may have had a history of motion before the Deccan rocks were emplaced, as discussed below.

The relatively thin layer of sediments in the plain to the south of the fault, as indicated by the basalt outcrops in the river beds at Shahada and Prakasha, is likely to be the result of the elevation of the plain (100–200 m) relative to the nearby Arabian Sea. Although the faulting we describe results in the subsidence of the plain, the proximity to a significantly lower base level is likely to prevent significant volumes of sediment from accumulating, which are instead transported and deposited in the ocean. The proximity to the oceanic base level suggests that in times of changing erosion levels the sediment-bedrock divide on the sides of the Tapti river valley could fluctuate in elevation.

4.2. The Drainage Pattern of India

The Tapti river is notable as being one of only two rivers, along with the nearby Narmada, with mouths on the west coast of India that have a significant catchment in the central part of the subcontinent (Figure 1). Further south, the drainage divide of the Indian peninsula is close to the west coast, along the spine of the Western Ghats (dotted line in Figure 1). The Narmada river is thought to follow its present course due to the long history of deformation on the Narmada-Son fault system [e.g., *West*, 1962; *Choubey*, 1971; *Biswas*, 1982], which follows the courses of these two rivers across the Indian subcontinent (marked *N* and *S* in Figure 1). It is likely that motion on the Tapti Fault is responsible for the westward flow of the Tapti river and its large catchment in central India. The subsiding footwall of the Tapti Fault is currently at an elevation of 100–200 m, which is lower than most of the central Indian plateau (∼500 m) and the spine of the Western Ghats along the west coast of India (500–1000 m). Motion on the fault, lowering the elevation of the west Indian drainage divide to below the level of central India, therefore provides a mechanism for the diversion of rivers from central India into the Arabian Sea and the establishment of a large, west flowing catchment. The topography and drainage pattern of India therefore suggest that the Tapti Fault has experienced more displacement than any other post-Deccan dip-slip faults that may cut the Western Ghats escarpment further to the south, where the drainage divide is close to the west coast.

The effects of uplift in the hanging wall of the Tapti Fault can be seen in the incision of the Narmada river. Where this river approaches within ∼30 km of the Tapti Fault, it incises a deep (up to ∼500 m) and narrow valley (Figure 2). In contrast, to the east and west it flows through a wide river valley. Given the low rates of strain within India, and so the low rate of slip on the Tapti Fault (discussed in more detail below), it is unsurprising that a river with a catchment the size of the Narmada is able to incise rapidly enough to keep pace with the rate of uplift of the Tapti Fault and retain its course.

In an insightful work, early in the history of studies of active deformation, *Vredenburg* [1906] suggested the presence of recent deformation in the region of the Narmada and Tapti rivers based upon irregularities in their gradients. The steep, almost linear gradient noted by *Vredenburg* [1906] in the lower reaches of the Narmada river can now be seen to include the area of the river course being affected by the uplifting hanging wall of the Tapti Fault (Figure 2a). The effects of active faulting are therefore expressed as irregularities in the gradients of rivers in India, which had been recognized as early as the mid-nineteenth century [*Medlicott*, 1860] and attributed to Quaternary deformation in the early twentieth century [*Vredenburg*, 1906].

5. Discussion

This paper has described field and remote sensing observations of Holocene-aged fault slip on the Tapti Fault in the Indian peninsula. We suggest that scarps crossing alluvial fans formed in one or more thrust-faulting earthquakes with magnitudes of 7.6–8.4. The large-scale geomorphology demonstrates the effect of the faulting on both the growth of the local mountain range and the continent-scale organization of river systems. Here we discuss the implications of our results for the tectonics and material properties of the Indian lithosphere.

5.1. Fault Properties and Scaling

A clear manifestation of the thickness of the seismogenic layer in peninsular India (40–50 km; e.g., *Mukherjee* [1942]; *Chen and Molnar* [1990]; *Chen and Kao* [1996]; *Mitra et al.* [2005]; *Craig et al.* [2012]) is provided by the distance over which topography and active uplift (marked by river incision) decay away from the Tapti Fault (∼50 km; Figure 2). The pattern of a thicker seismogenic layer resulting in longer-wavelength displacements surrounding a fault has been previously discussed [e.g., *Jackson and White*, 1989; *Scholz and Contreras*, 1998], and the Tapti Fault is consistent with this pattern.

The length of Tapti Fault scarp, and the vertical displacement of the fan surfaces, place constraints on the behavior and properties of the fault. Although there is no clear segmentation visible in the topography north of the fault, the fan offsets only exist along roughly the western half of the fault. As described above, the Quaternary geology is indistinguishable between the eastern and western parts of the fault, but there is no evidence for offsets in the fan surfaces on the eastern section. The along-strike length of the area with fan offsets is ∼40–50 km. This distance is similar to the thickness of the seismogenic layer in peninsular India [e.g., *Mukherjee*, 1942; *Chen and Molnar*, 1990; *Chen and Kao*, 1996; *Mitra et al.*, 2005; *Craig et al.*, 2012]. This along-strike limit in the fan offsets may arise from a possible approximate scaling between the downdip width of dip-slip faults and the along-strike extent of fault rupture segments. Such a relation has been suggested based on the segmentation of faults [e.g., *Wallace*, 1989] and is often observed in the slip patches of earthquakes in a range of tectonic settings [e.g., *Wald et al.*, 1996; *Ji et al.*, 2003; *Avouac et al.*, 2006; *Cheloni et al.*, 2010; *Copley et al.*, 2012; *Elliott et al.*, 2013], including individual high-slip patches in some subduction zone thrust events [e.g., *Chlieh et al.*, 2007; *Delouis et al.*, 2010].

The observed Holocene fan offsets also allow us to place constraints upon the material properties of the fault. Displacements of ~10–15 m are present along a ~40–50 km length of fault, implying a displacement-length ratio of ~3–5 $\times$ 10^{-4} if the offsets were produced in a single event on a plane dipping at 45°. This ratio is considerably larger than that usually observed in earthquakes (~ 5 $\times$ 10^{-5}; *Scholz* [1982]) but similar to that in the 2001 Bhuj and 1897 Assam earthquakes (Figure 1) and other intraplate events [e.g., *Scholz et al.*, 1986]. These results imply that earthquakes in the Indian peninsula are capable of generating large amounts of slip for a given rupture area, equivalent to having a high stress drop (35 $\pm$ 10 MPa in the case of Bhuj [*Copley et al.*, 2011]). This high stress drop may be related to the large seismogenic thickness, and so the high normal stresses experienced by the deeper parts of the faults, or to the low slip rates in the Indian peninsula resulting in frictional properties that are different from those of more rapidly slipping faults.

If the scarp offsets we have examined were formed in more than one earthquake, we can obtain a similar conclusion regarding the slip gradients, and therefore shear stress, that the fault can support. The eastern part of the fault has not ruptured since the fan deposition, despite the presence of ~10–15 m of vertical offset on the western part. This observation implies that the fault must be able to support displacement gradients of ~ 10^{-4} without the slip on the western part of the fault causing rupture on the eastern part, implying fault stresses of tens of megapascals.

5.2. The Forces Driving Faulting Within Peninsular India

Two main causes have been suggested for the faulting in peninsular India. *Bilham et al.* [2003] suggest that the flexure of the Indian lithosphere as it underthrusts the Tibetan Plateau can cause sufficient stresses to modulate the occurrence of earthquakes far into the Indian peninsula to the south, in a series of flexural waves. Similarly, *Vita-Finzi* [2004] proposed that the buckling of the Indian lithosphere controls the spatial distribution of seismicity. Alternatively, it has been suggested that the buoyancy force that is exerted upon the Indian peninsula due to the difference in crustal thickness between India and the Tibetan Plateau (or, equivalently, the force applied by India to the Tibetan Plateau to build and support the mountains), is sufficient to drive faulting within the Indian peninsula, without the locations of earthquake being modulated by flexure except beneath the Ganges basin [e.g., *Gowd et al.*, 1992; *Copley et al.*, 2011]. Both of these mechanisms would be expected to result in dip-slip faulting along planes roughly parallel to the overall strike of the southern margin of Tibet, as is observed in the seismicity of India. The exceptions to this pattern are in NE India, where the stress state may be more complex due to the subduction beneath the Indo-Burman Ranges of oceanic lithosphere attached to continental India, and in southern India where two oblique strike-slip events have been recorded. In northeast and southern India the strike-slip faulting has *P* axes oriented roughly perpendicular to the overall strike of the Himalayas (similar to the thrust faulting) and *T* axes striking ~E-W.

One method of attempting to assess the relative importance of the possible causes of the deformation lies in the mechanisms of the earthquakes. Faulting in response to flexure would be expected to result in extension and compression at different depths within the mechanically strong part of the lithosphere. The net compressive force transmitted between India and the Tibetan Plateau would result in compression throughout the thickness of the lithosphere. Beneath the Ganges Basin, the presence of shallow normal faulting and deeper thrust faulting shows the influence of the bending stresses relating to the underthrusting of India beneath Tibet [e.g., *Bilham et al.*, 2003; *Craig and Copley*, 2014, and references therein]. However, further south within India ~N-S compression is observed throughout the thickness of the seismogenic layer (e.g., in the Bhuj mainshock and aftershocks [*Antolik and Dreger*, 2003; *Bodin and Horton*, 2004; *Mandal et al.*, 2006; *Copley et al.*, 2011] and in teleseismically recorded events throughout the peninsula; Figure 1 and references therein). This pattern implies that the net compressional forces relating to the India-Asia collision dominate over flexural effects in controlling the stress state in the lithosphere everywhere to the south of the Ganges basin. An alternative explanation is that flexural extensional stresses are supported by the ductile layer in regions experiencing thrust-faulting earthquakes, and our short observation period has resulted in us not observing shallow normal-faulting events south of the Ganges basin that may occur in the future. Although we cannot rule out this possibility, we think it less likely because of recent results regarding the rheology of the Indian lithosphere. The stress drop of the Bhuj earthquake, and the observation that the elastic thickness of continental regions is related to, and is usually less than, the seismogenic thickness, both independently imply that the seismogenic layer is supporting the bulk of the stresses transmitted through

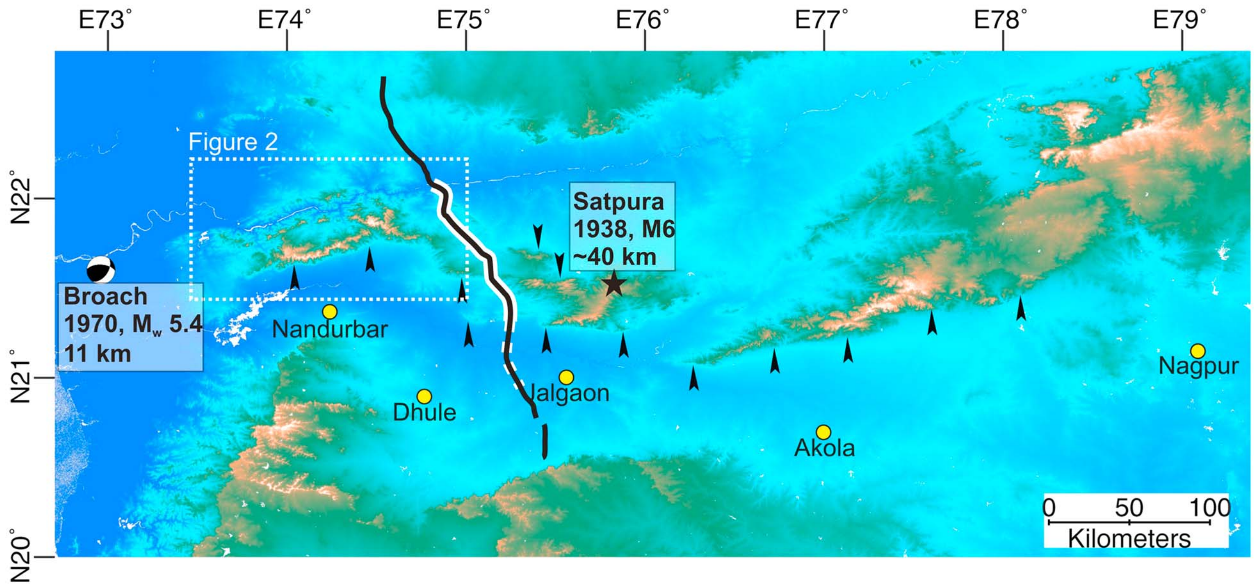

Figure 6. Topography of the area shown by the red dotted box in Figure 1. The region of the Tapti Fault, shown in Figure 2, is marked by the white box. The epicenters of the Broach and Satpura earthquakes are marked, along with cities in the region. The black arrows mark the locations of features visible in the landscape that are likely to be underlain by active faults, as discussed in the text. The black line shows the seismic survey analyzed by *Kaila et al.* [1989] and *Sridhar and Tewari* [2001]. The section of the line with a white border shows where those studies found ~2 km thick subbasalt sediments, and the section flanked by dashed white lines indicates where *Kaila et al.* [1989] suggested the subbasalt sediments were 0.5–1 km thick and *Sridhar and Tewari* [2001] believe they are absent.

the Indian lithosphere [e.g., *Copley et al.*, 2011; *Jackson et al.*, 2008]. However, we note that our interpretation of the dominant driving forces for the faulting in peninsular India is influenced by these previous studies.

5.3. Rate of Fault Slip and Likely Recurrence Intervals

It is likely that the fan offsets we have observed formed in one earthquake, or a small number of events, meaning we cannot use the presumed Holocene age of the fans to estimate the long-term slip rate of the fault. GPS measurements from within peninsular India can provide an upper bound on the fault slip rate at the present day, if we assume that all the geodetically allowable N-S shortening (~ 2 ± 1 mm/yr; *Bettinelli et al.* [2006]; *Banerjee et al.* [2008]) is concentrated onto the fault we have studied. This estimate is ~ 3 ± 1.4 mm/yr (assuming a fault dip of 45°). A lower bound on the slip rate can be obtained by using our estimated post-Deccan vertical fault offset (500–1500 m) and the age of emplacement of the volcanics (~65 Ma; *Hofmann et al.* [2000]), which is ~0.01 mm/yr (assuming a fault dip of 45°). These slip rates correspond to the recurrence interval for a single event producing the fan offsets we have observed of 5000 to 2 million years. We note that this estimate corresponds to repeated slip on a single plane, although the next section of fault likely to rupture in this region is along strike from the area of fan offsets, where there was no evidence for faulting during the Holocene.

5.4. The Spatial Continuation of Faulting in Central India

Here we discuss the lateral terminations of the Tapti Fault. The displacement on the fault (~0.5–1.5 km) is too large for the displacement gradients at the ends of the fault to be supported by elastic strains. One possible alternative is that the fault rotates about a vertical axis, and the displacement is accommodated on faults with slip that dies out toward rotation poles at their ends, such as has been discussed elsewhere for strike-slip faults (e.g., Mongolia and Iran) [*Bayasgalan et al.*, 1999; *Berberian et al.*, 2000]. Alternatively, the fault could simply link into other structures that transfer the motion to the boundaries of the Indian plate.

Figure 6 shows the series of ~E-W trending ridges that make up the Satpura mountain range (the area of coverage is shown in Figure 1), of which the uplifting hanging wall of the Tapti Fault forms the western part (inside the dotted white box in Figure 6). To the east of the Tapti Fault lie a series of mountain ranges that rise above the surrounding valleys and are at a higher elevation than the central Indian plateau to the north and south (Figure 1). In many places these ranges have linear margins and asymmetric shapes and contain within them high-elevation and low-relief landscapes showing signs of rapid erosion on their margins. These

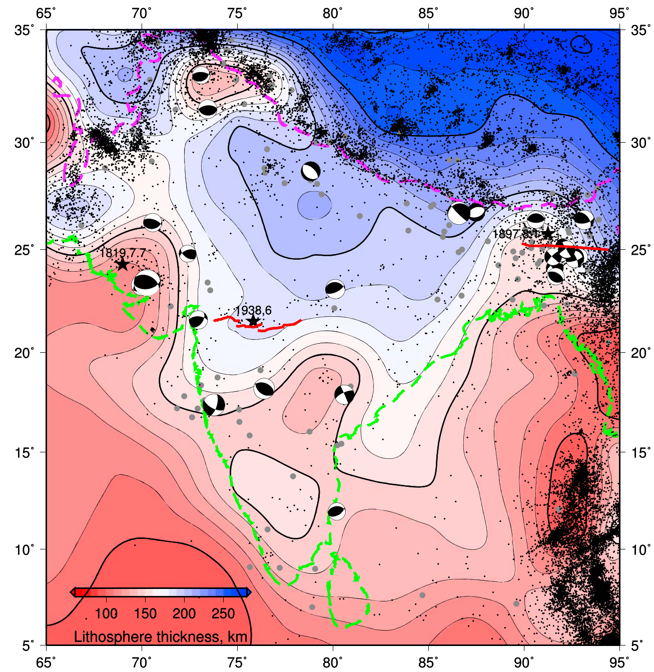

Figure 7. Lithosphere thickness from *Priestley and McKenzie* [2013], along with the earthquakes shown in Figure 1. Black dots show all events in the International Seismological Centre catalogue with magnitude greater than 3.0 [*International Seismological Centre*, 2014]. Grey circles show earthquakes prior to 1970 in the catalogue of *Szeliga et al.* [2010], dating back to the mid-eighteenth century. Red lines represent the active faulting in western India shown in Figure 6 and the Dauki fault along the southern margin of the Shillong plateau (the 1897 event ruptured the Oldham fault along the northern side of the range; *Bilham and England* [2001]). The green line shows the coastline, and the purple line the 1600 m contour on topography smoothed with a gaussian filter of width 100 km. The thick and thin contours of lithosphere thickness are at intervals of 50 km and 10 km.

topographic features are in contrast to the central Indian plateau to the north and south, which is largely flat, with little incision of drainage, and has edges that are curved on all scales up to hundreds of kilometers (e.g., the topography on the northern and southern edges of Figure 6 at 75°–77° longitude). The characteristics of the landscape lead us to suggest that the topographic fronts marked by black arrows in Figure 6 are likely to be underlain by active faults, which represent the continuation to the east of the displacement on the Tapti Fault. We have not examined these locations in the field, which is beyond the scope of this study, but the large-scale geomorphology suggests that a closer examination is warranted.

The presence of the thinned continental margin to the west of the Tapti Fault prevents us from making clear geomorphological interpretations of the faulting in that area, as large areas are below sea level or blanketed by thick sediment. The faulting may link with the Rann of Kachchh to the northwest, where magnitude 7 earthquakes occurred in 1819 and 2001 (Figure 1), but we currently lack the information to examine if this is the case.

5.5. Relationship of Faulting and Lithosphere Structure

Kaila et al. [1989] and *Sridhar and Tewari* [2001] used data from a seismic survey to study the crustal structure along a line that crosses the faulting east of the Tapti Fault, shown as a black line in Figure 6. In the central section of the line, shown white in Figure 6, they suggest the presence of ~2 km of low-velocity sediments beneath the Deccan basalts, with abrupt lateral boundaries. Based on the abruptness of the edges of this sedimentary package, it has been interpreted as the infill of a fault-bounded rift valley, part of the Narmada-Son Lineament system of faults. This fault system, thought to have been active numerous times since the Precambrian [e.g., *West*, 1962; *Choubey*, 1971; *Biswas*, 1982], is thought to have experienced normal faulting and sedimentation during the Cretaceous [*Biswas*, 1987]. The area of thick pre-Deccan sediments corresponds to the location being uplifted by the thrust faulting described in the previous section (Figure 6). The spatial correlation between the rift sediments and the region of present-day uplift by thrust faulting is highly suggestive of the thrust faults having reactivated preexisting basin-bounding normal faults. This situation is similar to that seen in other areas of peninsular India, such as the Rann of Kachchh, where thrusts are thought to have reactivated Mesozoic normal faults [e.g., *Talwani and Gangopadhyay*, 2001].

Figure 7 shows the thickness of the lithosphere in the Indian subcontinent (derived from the shear wave velocity by *Priestley and McKenzie* [2013]), along with recent and historical earthquakes, and the location of the faulting described in this paper. The 1918 Rann of Kachchh and 2001 Bhuj earthquakes occurred in a region with some of the thinnest lithosphere on the subcontinent. The Shillong Plateau, which is bounded by the fault that ruptured in the 1897 Assam earthquake and the Dauki Fault (marked in red in Figure 7) also lies in a region of relatively thin lithosphere. However, the faulting described in this paper, the 1997 Jabalpur event (at ∼ 23°N, 80°E), and a number of historical earthquakes (grey circles in Figure 7) have occurred in regions of significantly thicker lithosphere, even if events presumably related to bending beneath the Ganges foreland basin are neglected. Given the ∼250 km horizontal resolution of the surface wave tomography that *Priestley and McKenzie* [2013] used to estimate the thickness of the lithosphere, Figure 7 may suggest that earthquakes are more common close to gradients in lithosphere thickness, although this possibility is tentative. Such a situation is observed in other areas, such as the NE Baikal rift [*Sloan et al.*, 2011], and is thought to relate to inherited strength contrasts dating from before the areas of contrasting lithosphere were juxtaposed or created during that motion. However, our short observation time relative to the probable repeat times of earthquakes in the subcontinent prevents us from drawing any firm conclusions from the earthquake distribution in this regard.

Regardless of whether or not earthquakes are more common close to gradients in the lithosphere thickness, a notable feature of Figure 7 is that the lithosphere varies in thickness by over ∼60 km between areas experiencing some degree of active faulting. Such a variation would be expected to have a significant effect on the temperature, and therefore strength, of the lithospheric mantle. Faulting in areas with contrasting lithosphere thicknesses, and the reactivation of a rift in the region of the Tapti Fault, suggests two possibilities. The first is that narrow zones of thin lithosphere exist along old geological boundaries, have a strong control on the strength of the lithosphere, but are invisible to surface wave tomography (that of *Priestley and McKenzie* [2013], used to derive the lithosphere thickness shown in Figure 7, resolves features of scales ≥250 km). The second possibility is that the thickness of the lithospheric mantle may play a subservient role in controlling the distribution of faulting in India when compared to preexisting mechanical structures, such as faults and ductile shear zones. A similar situation to India is seen in east Africa, where the rift crosses between areas of thick and thin lithosphere but follows the course of Proterozoic mobile belts within the areas of thick lithosphere [e.g., *Ring*, 1994; *Ebinger et al.*, 1997; *Chorowicz*, 2005].

6. Conclusions

We have described active thrust faulting on the Tapti Fault in western India. One or more Holocene earthquakes, with moment magnitudes likely to be in the range 7.6–8.4, have offset alluvial fan surfaces. The displacement-length ratio of these offsets implies earthquakes with a stress drop on the order of tens of megapascals. The wide deformation zones caused by faulting in a region with a thick seismogenic layer have led to the construction of wide mountain ranges and valleys, and these valleys have shaped the continent-scale drainage pattern of India. The system of faults that bound the Satpura mountain range, including the Tapti Fault, are likely to have reactivated structures that experienced normal motion in the Mesozoic and pose a significant seismic hazard in central India.

Acknowledgments
We thank the District Collector of Nandurbar for logistical support during our fieldwork. This study forms part of the NERC- and ESRC-funded project "Earthquakes without Frontiers." We thank Mark Hoggard for maps of Indian rivers and Roger Bilham and one anonymous reviewer for comments on the manuscript. Topographic data in Figures 1, 2, 3a, 4a, and 6 are from the SRTM mission and freely available (e.g., at the USGS data center webpage). Satellite images in Figures 3b and 4b are from Google Earth. Photographs and elevation profiles were acquired during our fieldwork and can be obtained from the corresponding author upon request.

References

Adams, J., R. J. Wetmiller, H. S. Hasegawa, and J. Drysdale (1991), The first surface faulting from a historical intraplate earthquake in North America, *Nature*, *352*, 617–619.

Antolik, M., and D. S. Dreger (2003), Rupture process of the 26 January 2001 M_w 7.6 Bhuj, India, earthquake from teleseismic broadband data, *Bull. Seismol. Soc. Am.*, *93*, 1235–1248.

Assumpcao, M., and G. Suarez (1988), Source mechanisms of moderate-sized earthquake and stress orientation in mid-plate South America, *Geophys. J. Int.*, *92*, 253–267.

Avouac, J.-P., F. Ayoub, S. Leprince, O. Konca, and D. V. Helmberger (2006), The 2005, M_w 7.6 Kashmir earthquake: Sub-pixel correlation of ASTER images and seismic waveforms analysis, *Earth Planet. Sci. Lett.*, *249*, 514–528.

Banerjee, P., R. Burgmann, B. Nagarajan, and E. Apel (2008), Intraplate deformation of the Indian subcontinent, *Geophys. Res. Lett.*, *35*, L18301, doi:10.1029/2008GL035468.

Bayasgalan, A., J. Jackson, J.-F. Ritz, and S. Carretier (1999), Field examples of strike-slip fault terminations in Mongolia, and their tectonic significance, *Tectonics*, *18*, 394–411.

Berberian, M., J. A. Jackson, M. Qorashi, M. Talebian, M. Khatib, and K. Priestley (2000), The 1994 Sefidabeh earthquakes in eastern Iran: Blind thrust faulting and bedding-plane slip on a growing anticline, and active tectonics of the Sistan suture zone, *Geophys. J. Int.*, *142*, 283–299.

Bettinelli, P., J.-P. Avouac, M. Flouzat, F. Jouanne, L. Bollinger, P. Willis, and G. R. Chitrakar (2006), Plate motion of India and interseismic strain in the Nepal Himalaya from GPS and DORIS measurements, *J. Geod.*, *80*, 567–589.

Bilham, R. (1999), Slip parameters for the Rann of Kachchh, India, 16 June 1819 earthquake quantified from contemporary accounts, in *Coastal Tectonics*, vol. 146, edited by I. S. Stewart and C. Vita-Finzi, pp. 295–318, Geol. Soc. Spec. Publ., London, U. K.

Bilham, R., and P. England (2001), Plateau 'pop-up' in the great 1897 Assam earthquake, *Nature*, *410*, 806–809.

Bilham, R., R. Bendick, and K. Wallace (2003), Flexure of the Indian plate and intraplate earthquakes, *Proc. Indian Acad. Sci.*, *112*, 315–329.

Biswas, S. K. (1982), Rift basins in western margin of India and their hydrocarbon prospects with special reference to Kutch basin, *Bull. Am. Assoc. Petrol.*, *66*, 1497–1513.

Biswas, S. K. (1987), Regional tectonic framework, structure and evolution of the western marginal basins of India, *Tectonophysics*, *135*, 307–327.

Bodin, P., and S. Horton (2004), Source parameters and tectonic implications of aftershocks of the M_w 7.6 Bhuj earthquake of 26 January 2001, *Bull. Seismol. Soc. Am.*, *94*, 818–827.

Bruhat, L., S. Barbot, and J.-P. Avouac (2011), Evidence for postseismic deformation of the lower crust following the 2004 M_w6.0 Parkfield earthquake, *J. Geophys. Res.*, *116*, B08401, doi:10.1029/2010JB008073.

Chandra, U. (1977), Earthquakes of peninsular India: A seismotectonic study, *Bull. Seismol. Soc. Am.*, *67*, 1387–1413.

Chandrasekhar, D. V., D. C. Mishra, B. Singh, V. Vijayakumar, and R. Burgmann (2004), Source parameters of the Bhuj earthquake, India of January 26, 2001 from height and gravity changes, *Geophys. Res. Lett.*, *31*, L19608, doi:10.1029/2004GL020768.

Cheloni, D., et al. (2010), Coseismic and initial post-seismic slip of the 2009 M_w 6.3 L'Aquila earthquake, Italy, from GPS measurements, *Geophys. J. Int.*, *181*, 1539–1546.

Chen, W.-P., and H. Kao (1996), Seismotectonics of Asia: Some recent progress, in *The Tectonic Evolution of Asia*, edited by A. Yin and M. Harrison, pp. 37–62, Cambridge Univ. Press, New York.

Chen, W.-P., and P. Molnar (1990), Source parameters of earthquakes and intraplate deformation beneath the Shillong Plateau and the northern Indoburman ranges, *J. Geophys. Res.*, *95*, 12,527–12,552.

Chlieh, M., et al. (2007), Coseismic slip and afterslip of the great M_w 9.15 Sumatra-Andaman earthquake of 2004, *Bull. Seismol. Soc. Am.*, *97*, S152–S173.

Chorowicz, J. (2005), The East African rift system, *J. Afr. Earth Sci.*, *43*, 379–410.

Choubey, V. D. (1971), Narmada-Son lineament, India, *Nature*, *232*, 38–40.

Chung, W.-Y. (1993), Source parameters of two rift-associated intraplate earthquakes in peninsular India: The Bhadrachalam earthquake of April 13, 1969 and the Broach earthquake of March 23, 1970, *Tectonophysics*, *225*, 219–230.

Chung, W.-Y., and H. Gao (1995), Source parameters of the Anjar earthquake of July 21, 1956, India, and its seismotectonic implications for the Kutch rift basin, *Tectonophysics*, *424*, 281–292.

Copley, A., J.-P. Avouac, J. Hollingsworth, and S. Leprince (2011), The 2001 M_w 7.6 Bhuj earthquake, low fault friction, and the crustal support of plate driving forces in India, *J. Geophys. Res.*, *116*, B08405, doi:10.1029/2010JB008137.

Copley, A., J. Hollingsworth, and E. Bergman (2012), Constraints on fault and lithosphere rheology from the coseismic slip and postseismic afterslip of the 2006 M_w7.0 Mozambique earthquake, *J. Geophys. Res.*, *117*, B03404, doi:10.1029/2011JB008580.

Craig, T., and A. Copley (2014), An explanation for the age independence of oceanic elastic thickness estimates from flexural profiles at subduction zones, and implications for continental rheology, *Earth Planet. Sci. Lett.*, *392*, 207–216.

Craig, T., A. Copley, and J. Jackson (2012), Thermal and tectonic consequences of India underthrusting Tibet, *Earth Planet. Sci. Lett.*, *353–354*, 231–239.

Delouis, B., J.-M. Nocquet, and M. Vallee (2010), Slip distribution of the February 27, 2010 M_w = 8.8 Maule earthquake, central Chile, from static and highrate GPS, InSAR, and broadband teleseismic data, *Geophys. Res. Lett.*, *37*, L17305, doi:10.1029/2010GL043899.

Ebinger, C., Y. Poudjom Djomani, E. Mbede, A. Foster, and J. B. Dawson (1997), Rifting Archean lithosphere: The Eyasi-Manyara-Natron rifts, East Africa, *J. Geol. Soc.*, *154*, 947–960.

Elliott, J., A. Copley, R. Holley, K. Scharer, and B. Parsons (2013), The 2011 M_w 7.1 Van (Eastern Turkey) earthquake, *J. Geophys. Res. Solid Earth*, *118*, 1619–1637, doi:10.1002/jgrb.50117.

Farr, T. G., and M. Kobrick (2000), Shuttle radar topography mission produces a wealth of data, *Eos Trans. AGU*, *81*(48), 583–585.

Geological Survey of India (2000), *Seismotectonic Atlas of India and Its Environs*, GSI, Kolkata, India.

Gibling, M. R., S. K. Tandon, R. Sinha, and M. Jain (2005), Discontinuity-bounded alluvial sequences of the southern Gangetic plains, India: Aggradation and degradation in response to monsoonal strength, *J. Sediment. Res.*, *75*, 369–385.

Gowd, T. N., S. V. Srirama Rao, and V. K. Gaur (1992), Tectonic stress field in the Indian subcontinent, *J. Geophys. Res.*, *97*, 11,879–11,888.

Hofmann, C., G. Feraud, and V. Courtillot (2000), ^{40}Ar/^{39}Ar dating of mineral separates and whole rocks from the Western Ghats lava pile: Further constraints on the duration and age of the Deccan traps, *Earth Planet. Sci. Lett.*, *180*, 13–27.

International Seismological Centre (2014), *On-Line Bulletin*, Int. Seis. Cent., Thatcham, U. K. [http://www.isc.ac.uk.]

Jackson, J., D. McKenzie, K. Priestley, and B. Emmerson (2008), New views on the structure and rheology of the lithosphere, *J. Geol. Soc.*, *165*, 453–465.

Jackson, J. A. (2002), Faulting, flow, and the strength of the continental lithosphere, *Int. Geol. Rev.*, *44*, 39–61.

Jackson, J. A., and N. J. White (1989), Normal faulting in the upper continental crust: Observations from regions of active extension, *J. Struct. Geol.*, *11*, 15–36.

Jain, M., and S. K. Tandon (2003), Fluvial response to Late Quaternary climate changes, western India, *Quat. Sci. Rev.*, *22*, 2223–2235.

Jain, S. C., K. K. K. Nair, and D. B. Yaedekar (1995), *Project Crumansonata: Geoscientific Studies of the Son-Narmada-Tapti Lineament Zone, Chapter Geology of the Son-Narmada-Tapti Lineament Zone in Central India*, pp. 1–154, Geological Survey of India, Kolkata, India.

Jaupart, C., and J. C. Mareschal (1999), The thermal thickness of continental roots, *Lithos*, *48*, 93–114.

Ji, C., D. V. Helmberger, D. J. Wald, and K.-F. Ma (2003), Slip history and dynamic implications of the 1999 Chi-Chi, Taiwan, earthquake, *J. Geophys. Res.*, *108*(B9), 2412, doi:10.1029/2002JB001764.

Johnston, A. C. (1996), Seismic moment assessment of earthquakes in stable continental regions: 1. Instrumental seismicity, *Geophys. J. Int.*, *124*, 381–414.

Johnston, A. C., and E. S. Schweig (1996), The enigma of the New Madrid earthquakes of 1811–1812, *Annu. Rev. Earth Planet. Sci.*, *24*, 339–384.

Jolivet, M., et al. (2007), An uplifted, flat, old but still preserved erosion surface, *Geology*, *35*, 871–874.

Kaila, K. L., I. B. P. Rao, P. R. Rao, N. M. Rao, V. G. Krishna, and A. R. Sridhar (1989), DSS studies over Deccan Traps along the Thuadara-Sendhwa-Sindad profile, across Narmada-Son Lineament, India, in *Properties and Processes of Earth's Lower Crust*, vol. 51, pp. 127–141, AGU, Washington, D. C.

Kaufmann, G., and K. Lambek (2002), Glacial isostatic adjustment and the radial viscosity profile from inverse modeling, *J. Geophys. Res.*, *107*(B11), 2280, doi:10.1029/2001JB000941.

Langston, C. A. (1976), A body wave inversion of the Koyna, India, earthquake of December 10, 1967, and some implications for body wave focal mechanisms, *J. Geophys. Res.*, *81*, 2517–2529.

Mackwell, S. J., M. E. Zimmerman, and D. L. Kohlstedt (1998), High temperature deformation of dry diabase with application to the tectonics of Venus, *J. Geophys. Res.*, *103*, 975–984.

Maggi, A., J. A. Jackson, D. P. McKenzie, and K. F. Priestley (2000a), Earthquake focal depths, effective elastic thickness, and the strength of the continental lithosphere, *Geology*, *28*, 495–498.

Maggi, A., J. A. Jackson, K. Priestley, and C. Baker (2000b), A re-assessment of focal depth distributions in southern Iran, the Tien Shan and northern India: Do earthquakes really occur in the continental mantle?, *Geophys. J. Int.*, *143*, 629–661.

Mandal, P., R. Narsaiah, B. Sairam, C. Satyamurty, and I. P. Raju (2006), Relocation of early and late aftershocks of the 2001 Bhuj earthquake using joint hypocentral determination (JHD) technique: Implication toward the continued aftershock activity for more than four years, *Pure Appl. Geophys.*, *163*, 1561–1581.

Martin, S., and W. Szeliga (2010), A catalog of felt intensity data for 570 earthquakes in India from 1636 to 2009, *Bull. Seismol. Soc. Am.*, *100*, 562–569.

McCaffrey, R. (1989), Teleseismic investigation of the January 22, 1988 Tennant Creek, Australia, earthquakes, *Geophys. Res. Lett.*, *16*, 413–416.

Medlicott, J. G. (1860), On the geological structure of the central portion of the Nerbudda District, *Mem. Geol. Surv. India*, *2*, 97–278.

Mitra, S., K. Priestley, A. K. Bhattacharyya, and V. K. Gaur (2005), Crustal structure and earthquake focal depths beneath northeastern India and southern Tibet, *Geophys. J. Int.*, *160*, 227–248.

Molnar, P., W.-P. Chen, T. J. Fitch, P. Tapponnier, W. E. K. Warsi, and F. Wu (1977), Structure and tectonics of the Himalaya: A brief summary of relevant geophysical observations, in *Himalaya; Sciences de la Terre: Centre Nationale de la Reecherche Scientifique, Colloques Internationaux du CNRS*, vol. 268, pp. 269–294, Editions du Centre Nationale de la Reecherche Scientifique, Paris.

Mukherjee, S. M. (1942), Seismological features of the Satpura earthquake of the 14th March 1938, *Proc. Indian Acad. Sci. Sec. A*, *16*, 167–175.

Neilson, G., R. M. W. Musson, and P. W. Burton (1984), The 'London' earthquake of 1580, April 6, *Eng. Geol.*, *20*, 113–141.

Ni, J., and M. Barazangi (1984), Seismotectonics of the Himalayan collision zone: Geometry of the undershrusting Indian plate beneath the Himalaya, *J. Geophys. Res.*, *89*, 1147–1163.

Philip, H., E. Rogozhin, A. Cisternas, J. C. Bousquet, B. Borisov, and A. Karakhanian (1992), The Armenian earthquake of 1988 December 7: Faulting and folding, neotectonics and palaeoseismicity, *Geophys. J. Int.*, *110*, 141–158.

Priestley, K., and D. McKenzie (2013), The relationship between shear wave velocity, temperature, attenuation and viscosity in the shallow part of the mantle, *Earth Planet. Sci. Lett.*, *381*, 78–91.

Priestley, K., J. Jackson, and D. McKenzie (2008), Lithospheric structure and deep earthquakes beneath India, the Himalaya and southern Tibet, *Geophys. J. Int.*, *172*, 345–362.

Rajendran, C. P. (2000), Using geological data for earthquake studies: A perspective from peninsular India, *Curr. Sci.*, *79*, 1251–1258.

Rao, B., and P. Rao (1984), Historical seismicity of peninsular India, *Bull. Seismol. Soc. Am.*, *74*, 2519–2533.

Rao, B. R. (2000), Historical seismicity and deformation rates in the Indian peninsular shield, *J. Seismol.*, *4*, 247–258.

Ring, U. (1994), The influence of preexisting structure on the evolution of the Cenozoic Malawi rift (East African rift system), *Tectonics*, *13*, 313–326.

Schmidt, D. A., and R. Burgmann (2006), InSAR constraints on the source parameters of the 2001 Bhuj earthquake, *Geophys. Res. Lett.*, *33*, L02315, doi:10.1029/2005GL025109.

Scholz, C. (1982), Scaling laws for large earthquakes: Consequence for physical models, *Bull. Seismol. Soc. Am.*, *72*, 1–14.

Scholz, C. H., and J. C. Contreras (1998), Mechanics of continental rift architecture, *Geology*, *26*, 967–970.

Scholz, C. H., C. Aviles, and S. Wesnousky (1986), Scaling differences between large intraplate and interplate earthquakes, *Bull. Seismol. Soc. Am.*, *76*, 65–70.

Schulte, S. M., and W. D. Mooney (2005), An updated global earthquake catalogue for stable continental regions: Reassessing the correlation with ancient rifts, *Geophys. J. Int.*, *161*, 707–721.

Seeber, L., G. Ekstrom, S. K. Jain, C. V. R. Murty, N. Chandak, and J. G. Armbruster (1996), The 1993 Killari earthquake in central India: A new fault in Mesozoic basalt flows?, *J. Geophys. Res.*, *101*, 8543–8560.

Simons, F. J., and R. D. van der Hilst (2002), Age-dependent seismic thickness and mechanical strength of the Australian lithosphere, *Geophys. Res. Lett.*, *29*(11), 24-1–24-4, doi:10.1029/2002GL014962.

Sloan, R. A., J. A. Jackson, D. McKenzie, and K. Priestley (2011), Earthquake depth distributions in central Asia, and their relations with lithospheric thickness, shortening and extension, *Geophys. J. Int.*, *185*, 1–29.

Sridhar, A. R., and H. C. Tewari (2001), Existence of a sedimentary graben in the western part of the Narmada Zone: Seismic evidence, *J. Geodyn.*, *31*, 19–31.

Srivastava, P., N. Juyal, A. K. Singhvi, R. J. Wasson, and M. D. Bateman (2001), Luminescence chrnology of river adjustment and incision of Quaternary sediments in the alluvial plain of the Sabarmati River, north Gujarat, India, *Geomorphology*, *36*, 217–229.

Sykes, L. R. (1978), Intraplate seismicity, reactivation of preexisting zones of weakness, alkaline magmatism, and other tectonism postdating continental fragmentation, *Rev. Geophys. Space Phys.*, *16*, 621–688.

Szeliga, W., S. Hough, S. Martin, and R. Bilham (2010), Intensity, magnitude, location, and attenuation in India for felt earthquakes since 1762, *Bull. Seismol. Soc. Am.*, *100*, 570–584.

Talwani, P., and A. Gangopadhyay (2001), Tectonic framework of the Kachchh earthquake of January 26, 2001, *Seismol. Res. Lett.*, *72*, 336–345.

Vita-Finzi, C. (2004), Buckle-controlled seismogenic faulting in peninsular India, *Quat. Sci. Rev.*, *23*, 2405–2412.

Vredenburg, E. (1906), Pleistocene movement as indicated by irregularities of gradient of the Narbada and other rivers in the Indian peninsular, *Rec. Geol. Surv. India*, *33*, 33–45.

Wald, D. J., T. H. Heaton, and K. W. Hudnut (1996), The slip history of the 1994 Northridge, California, earthquake determined from strong-motion, teleseismic, GPS, and leveling data, *Bull. Seismol. Soc. Am.*, *86*, 49–70.

Wallace, R. E. (1989), Fault-plane segmentation in brittle crust and anisotropy in loading system, *U.S. Geol. Surv. Open File Rep., 89-315*, pp. 400–408.

Wesnousky, S. G., L. Seeber, T. K. Rockwell, V. Thakur, R. Briggs, S. Kumar, and D. Ragona (2001), Eight days in Bhuj: Field report bearing on surface rupture and genesis of the 26 January 2001 Republic Day earthquake of India, *Seismol. Res. Lett.*, *72*, 514–524.

West, W. D. (1962), The line of Narmada-Son valley, *Curr. Sci.*, *31*, 143–144.

Williams, M. A. J., J. N. Pal, M. Jaiswal, and A. K. Singhvi (2006), River response to Quaternary climatic fluctuations: Evidence from the Son and Belan valleys, north-central India, *Quat. Sci. Rev.*, *25*, 2619–2631.

Yielding, G. H., J. A. Jackson, G. C. P. King, H. Sinvhal, C. Vita-Finzi, and R.-M. Wood (1981), Relations between surface deformation, fault geometry, seismicity, and rupture characteristics during the El Asnam (Algeria) earthquake of 10 October 1980, *Earth Planet. Sci. Lett.*, *56*, 287–304.